

# From Chaos to Pseudo-Randomness: A Case Study on the 2D Coupled Map Lattice

Yong Wang, Zhuo Liu, Leo Yu Zhang, *Member, IEEE*, Fabio Pareschi, *Senior Member, IEEE*, Gianluca Setti, *Fellow, IEEE* and Guanrong Chen, *Life Fellow, IEEE*

**Abstract**—Applying chaos theory for secure digital communications is promising and it is well acknowledged that in such applications the underlying chaotic systems should be carefully chosen. However, the requirements imposed on the chaotic systems are usually heuristic, without theoretic guarantee for the resultant communication scheme. Among all the primitives for secure communications, it is well-accepted that (pseudo) random numbers are most essential. Taking the well-studied two-dimensional coupled map lattice (2D CML) as an example, this paper performs a theoretical study towards pseudo-random number generation with the 2D CML. In so doing, an analytical expression of the Lyapunov exponent (LE) spectrum of the 2D CML is first derived. Using the LEs, one can configure system parameters to ensure the 2D CML only exhibits complex dynamic behavior, and then collect pseudo-random numbers from the system orbits. Moreover, based on the observation that least significant bit distributes more evenly in the (pseudo) random distribution, an extraction algorithm E is developed with the property that, when applied to the orbits of the 2D CML, it can squeeze uniform bits. In implementation, if fixed-point arithmetic is used in binary format with a precision of  $z$  bits after the radix point, E can ensure that the deviation of the squeezed bits is bounded by  $2^{-z}$ . Further simulation results demonstrate that the new method not only guide the 2D CML model to exhibit complex dynamic behavior, but also generate uniformly distributed independent bits. In particular, the squeezed pseudo-random bits can pass both NIST 800-22 and TestU01 test suites in various settings. This study thereby provides a theoretical basis for effectively applying the 2D CML to secure communications.

**Index Terms**—Chaos; Lyapunov Exponent; Random Number Generator; Secure Communication; 2D Coupled Map Lattice.

## I. INTRODUCTION

IN THE past two decades, chaotic systems have been widely used for secure communications, primarily due to their special properties such as complexity, pseudo-randomness and ergodicity [1, 2]. Many encryption algorithms and secure communication schemes based on chaotic systems have been proposed, creating a great deal of research across nonlinear dynamics and information security [3–6]. Essentially, the inherent properties of chaotic systems play an important role in ensuring the security of the schemes. Therefore, selecting

or constructing a chaotic system from the perspective of cryptographic applications has become an important issue in the research of chaos-based secure communications.

There are two views on how to choose chaotic systems for secure communications [7]. The first one is to choose simple chaotic systems since, in general, simple chaotic systems have fewer arithmetic operations, and thus less computational complexity. Secure communication schemes based on such systems typically have better runtime efficiency [6, 8]. However, if the structure of a simple chaotic system is not complicated enough, an attacker might be able to predict its chaotic orbits, which are used for secure communication directly or indirectly [9, 10]. This probably brings some potential vulnerability to the secure communication schemes.

To alleviate this problem, on the one hand, one may consider enhancing the dynamic complexity of simple chaotic systems [11–14]. In this way, a better trade-off between security and efficiency of simple chaotic systems can be obtained. On the other hand, one may use higher-dimensional chaotic systems to design better secure communication schemes [15, 16]. Compared with simple chaotic systems, such as the logistic map and the tent map, a higher-dimensional chaotic system typically has more complicated dynamic behavior. Generally, it is much more difficult, if not impossible, to predict the sequences generated by a higher-dimensional chaotic system. However, the gain in security is not free, since more arithmetic operations of a higher-dimensional chaotic system will consume more computational capacity and lead to a lower running speed. To decrease the number of iterations of a higher-dimensional system and achieve higher efficiency, it is common to extract more pseudo-random bits from a single iteration of the higher-dimensional chaotic system [11, 17, 18]. But this is heuristic and depends on the pseudo-randomness of the underlying chaotic system.

Another method to improve efficiency is to iterate the higher-dimensional chaotic system in parallel. However, it only applies to higher-dimensional chaotic systems with a parallel structure.

Besides the consideration about the trade-off between security and efficiency, another critical issue is the effect of finite-precision representation of chaotic orbits [19]. In general, chaotic orbits are given by real numbers, and real numbers are truncated and represented in either floating-point or fixed-point arithmetic on digital computer. If expressed with a certain precision under the fixed-point arithmetic, all chaotic systems will inevitably degenerate to become periodic. Worse yet, if chaotic systems are not configured correctly, their orbits,

Y. Wang and Z. Liu are with the College of Computer Science and Technology, Chongqing University of Posts and Telecommunications, China (email: wangyong1@cqupt.edu.cn; liuzhuo1987@outlook.com).

L. Zhang is with the School of Information Technology, Deakin University, Australia (email: leo.zhang@deakin.edu.au).

F. Pareschi and G. Setti are with the Department of Electronics and Telecommunications, Politecnico di Torino, Italy (email: fabio.pareschi@polito.it; gianluca.setti@polito.it).

G. Chen is with the Department of Electrical Engineering, City University of Hong Kong, Hong Kong SAR (email: eegchen@cityu.edu.hk).

even represented by real numbers, could fall into periodic with a short period. Without deliberate design, therefore, these problems will degrade the security of chaos-based encryption algorithms. From this perspective, to design a fully-fledged chaotic secure communication system, it is necessary and imperative to have some theoretic guidelines for ensuring chaotic orbits to run in full chaotic state and the pseudo-random bits extracted from digitized orbits are evenly distributed with a sufficiently long period. The present work tries to address this issue by taking the two-dimensional coupled map lattice (2D CML) for a case study.

The coupled map lattice is a classic model of spatiotemporal chaos. It is a complex two-directional chaotic system coupled with multiple identical simple chaotic maps, and it has excellent scalability. All the nodes in the CML have the same structure, so their arithmetic operations can be computed individually. And it is possible to run the CML in parallel by some special design [20]. Moreover, since the CML consists of multiple nodes, it will degenerate to a periodic system only when all the nodes are in periodic state. From this point of view, under finite precision representation, the period of CML model is longer than that of a single node (a simple chaotic map) [21], which can easily make the orbital period to be long enough for practical applications.

Based on the above-mentioned merits, the potentials of CML have been exploited to design various secure communication algorithms in recent years [18, 22–24, 24–28]. For example, by using the CML as the core of diffusion operations, a cryptographic model is proposed to guarantee better security of information processes [22]. A novel pseudo-random number generator (PRNG) based on CML is proposed in [18], which has a high potential to be used for cryptographic applications. The sequences generated from CML provide a new way to construct nonlinear substitution boxes (S-boxes), which lays a good foundation for building excellent S-boxes [23]. In [24], the way of designing S-boxes based on CML is assembled to an image encryption algorithm to enhance the security. CML can also be easily mixed with other technologies, for example, DNA coding, to design better encryption algorithms [25]. From a theoretical perspective, to further enhance the complexity of dynamic behavior, the one-dimensional CML is extended to the two-dimensional form [26]. Some hash functions and encryption algorithms are heuristically developed based on the complexity, diffusion and randomness of the 2D CML [27, 28].

According to [29, 30], the state of a CML system (either 1D or 2D) can have different patterns, such as frozen random pattern, competition intermittency and fully developed chaos, when setting different values for the parameters of the CML. However, to the best of our knowledge, there are little theoretical analysis on the dynamics of 2D CML, although the 2D CML has already been heuristically applied to secure communications. Moreover, as mentioned above, heuristically extracting pseudo-random bits from chaotic orbits will leave a security loophole for the integrated system, which is also the case for the 2D CML.

To address these challenges, this paper studies the dynamics of 2D CML as well as pseudo-random bit generation from

orbits of 2D CML in a theoretical perspective. The main contributions of this work are summarized as follows:

- For a commonly used 2D CML system, the analytic formula between the Lyapunov exponents (LEs) and the parameters of the model is derived, which provides theoretical guarantee for ensuring the 2D CML to run in fully developed chaotic state.
- Focusing on the fixed-point arithmetic, an extraction algorithm **E** is introduced to process the digitized orbits of the 2D CML, which ensures the pseudo-random bits extracted from the orbits to be uniform. This extraction algorithm, concerning the acquisition of uniform bits from non-uniform random sources, is also of research interest in its own right.
- Extensive experiments are performed to verify the theoretical results. In particular, it is demonstrated that the extracted bits from the orbits of 2D CML successfully pass both NIST 800-22 and TestU01 tests [31, 32] under different settings.

The rest of the paper is organized as follows. Some preliminary knowledge is given in Sec. II. In Sec. III, theoretical Lyapunov exponent analysis of the 2D CML is presented and the practical question of how to extract uniform random bit from the orbits of the 2D CML is addressed. In Sec. IV, some numerical tests are presented to verify the theoretical results. Finally, conclusion is drawn in Sec. V.

## II. PRELIMINARIES

To prepare for the technical development of this work, some preliminary knowledge is provided in this section.

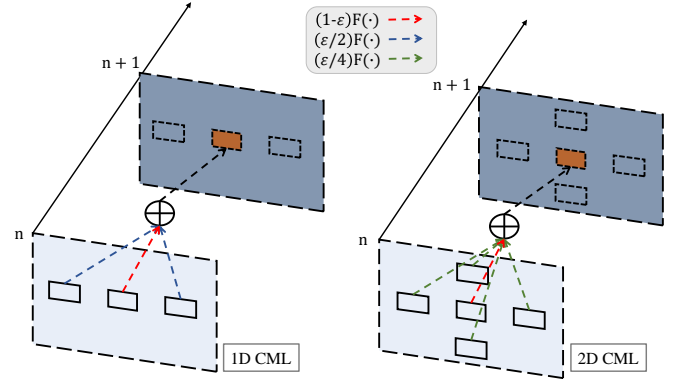


Fig. 1. The diagram of the 1D and 2D CML models.

### A. Two CML Models

The first CML model, as depicted in Fig. 1, is proposed by Kaneko in [29] and is one of the classic platform for studying spatiotemporal chaos.

**Definition 1.** [33] *The general one-dimensional nearest-neighbor CML model is described by*

$$x_{n+1}^u = (1 - \varepsilon)F(x_n^u) + \frac{\varepsilon}{2} [F(x_n^{u+1}) + F(x_n^{u-1})],$$

where  $n = 1, 2, \dots$ , is the time index,  $u = 1, 2, \dots, R$ , is the space index,  $x_n^u$  is the state value of the  $u$ -th node at time  $n$ ,

$\varepsilon \in (0, 1)$  is the coupling parameter, and  $F$  is a chaotic map. The periodic boundary condition is  $x_n^0 = x_n^R$ .

In the lattice, the coupling parameter  $\varepsilon$  between the nodes plays an important role in maintaining the complex dynamic behavior of the model. A tiny change in one node can affect other nodes and even be diffused to the whole lattice after some iterations. To further enhance the dynamic complexity, the one-dimensional CML model is extended to the two-dimensional version as follows.

**Definition 2.** The two-dimensional CML model is defined by

$$x_{n+1}^{u,v} = (1 - \varepsilon)F(x_n^{u,v}) + \frac{\varepsilon}{4} [F(x_n^{u+1,v}) + F(x_n^{u-1,v}) + F(x_n^{u,v+1}) + F(x_n^{u,v-1})], \quad (1)$$

where  $u = 1, 2, \dots, R$ , and  $v = 1, 2, \dots, L$ , are the row and column indexes of the nodes, respectively. The periodic boundary conditions are  $x_n^{u+R,v} = x_n^{u,v}$  and  $x_n^{u,v+L} = x_n^{u,v}$ .

### B. Lyapunov Exponent

Regarding nonlinear dynamic systems, the Lyapunov exponent (LE) is the key to measure chaotic behaviors. The maximum LE of the system  $x_{n+1} = F(x_n)$  is defined as [34]

$$\text{LE} = \lim_{n \rightarrow \infty} \frac{1}{n} \ln \left| \prod_{m=0}^n F'(x_m) \right|. \quad (2)$$

The value of LE is affected by the parameters in  $F$  and a positive LE indicates that the dynamic system is chaotic if its orbits are globally bounded. Moreover, the larger the LE is, the more complicated chaotic behavior the system has. For higher-dimensional systems or coupled systems like CML, it can have multiple LEs, and a strictly positive maximum LE indicates chaos.

For cryptographic confusion and diffusion suggested by Shannon [35], it is desirable to run a chaotic system with a large LE, so that any tiny change of the system parameters will spread out and be amplified gradually. For the requirement of pseudo-randomness [36], it is necessary to run the underlying chaotic system with large LE so as to minimize the correlation between orbits produced by proximal parameters.

### C. Non-uniform Randomness and Non-uniform Pseudo-Randomness

Let  $x_{n+1} = F(x_n)$  be an iterative chaotic system with value range  $(0, 1)$ . Given the initial condition and system parameters, the orbits of this system are said to follow a pseudo-random distribution. Conceptually, by iterating  $F$ , the distribution function of  $\{x_i\}_{i=0}^\infty$ ,  $D(F, x_0)$ , can be obtained.

**Definition 3.**  $D(F, x_0)$  is a pseudo-random distribution (PRD) if there exists a non-uniform true random distribution with the same density and there is no probabilistic polynomial-time (p.p.t.) algorithm that can distinguish them with a non-negligible probability.

In the studies of true random number generation, it is common to employ certain entropy extractor to squeeze uniform true random numbers from non-uniform true random

source [37]. While in the studies of pseudo-random number generation, there is no explicit tool that allows one to extract uniform pseudo-random bits (the functionality of PRNG) from a non-uniform pseudo-random source with an unknown distribution, and the introduction of PRD could be seen as one particular way to bridge this gap, as will be further discussed in Sec. III-B. In fact, it is easy to build a PRD by inversely sampling the output of a PRNG [38], but not vice versa. From this point of view, it is reasonable to believe that, like true random numbers obtained by squeezing non-uniform true random source, uniform pseudo-random numbers may be obtained by manipulating and compressing certain non-uniform PRD.

### D. Independence Test

**Definition 4.** Let  $x$  and  $y$  be two random variables that obey two random distributions, and  $x_i$  and  $y_i$  ( $i \in [1, K]$ ) be  $K$  independent observations of  $x$  and  $y$ , respectively. The Pearson correlation coefficient  $k_{xy}$  between  $x$  and  $y$  is

$$k_{xy} = \frac{\sum_{i=1}^K x_i y_i - K \bar{x} \bar{y}}{\sqrt{\left( \sum_{i=1}^K x_i^2 - K \bar{x}^2 \right) \left( \sum_{i=1}^K y_i^2 - K \bar{y}^2 \right)}},$$

where  $\bar{x} = \frac{1}{K} \sum_{i=1}^K x_i$  and  $\bar{y} = \frac{1}{K} \sum_{i=1}^K y_i$ .

If  $x$  and  $y$  are independent of each other, then Fisher's transformation of  $k_{xy}$ ,

$$D = \frac{\sqrt{K-3}}{2} \ln \left| \frac{1 + k_{xy}}{1 - k_{xy}} \right|,$$

will approximately follow the standard normal distribution. By setting a significance level  $\alpha$ , one can compare whether the empirical value  $D$  falls within the confidence interval  $(\Phi^{-1}(\alpha/2), -\Phi^{-1}(\alpha/2))$ , where  $\Phi$  is the cumulative distribution function of the standard normal distribution. For a more reliable result, multiple tests should be applied and other tests, such as the chi-square test of independence and Kolmogorov-Smirnov test, should also be used. More importantly, one can apply this kind of tests between a PRD and a true random distribution, provided that no p.p.t. algorithm can distinguish this PRD from a certain true random distribution. Also, the test can be applied to two PRDs if both of them cannot be distinguished from true random distributions.

## III. FROM CHAOS TO PSEUDO-RANDOMNESS

With the preliminary knowledge introduced above, a theoretic analysis of the 2D CML is presented in this section. Firstly, the analytical expression of all the LEs of the 2D CML is deduced in Sec. III-A, which will be used to enforce the system to run in fully developed chaotic state by using appropriate parameters. Secondly, it will discuss how to extract pseudo uniform bits with minimum bias from a pseudo-random distribution. Based on this result, an end-to-end extraction algorithm **E** will be designed to distill random bits from the orbits of 2D CML with theoretical support.

### A. Lyapunov Exponent Formula of the 2D CML

As stated in Sec. I, for either designing chaotic ciphers or producing random numbers, one should carefully set the parameters to make the chaotic system to operate in a fully developed chaotic mode. As stated in Sec. II-B, this can be accomplished by carefully selecting the parameter(s) of the chaotic system. Here, since LE is defined asymptotically as a limit, the synchronization of node values will be used to derive an analytical expression of all LEs for the 2D CML.

To begin with, convert the 2D CML model with  $R$  rows and  $L$  columns to a one-dimensional model by rearranging the nodes according to the order from left to right and from top to bottom. Thus, Eq. (1) is converted to

$$\begin{aligned} x_{n+1}^{(u-1)L+v} &= (1-\varepsilon)F(x_n^{(u-1)L+v}) + \frac{\varepsilon}{4} [F(x_n^{u \times L+v}) \\ &\quad + F(x_n^{(u-2)L+v}) + F(x_n^{(u-1)L+v+1}) \\ &\quad + F(x_n^{(u-1)L+v-1})]. \end{aligned} \quad (3)$$

Correspondingly, the periodic boundary conditions will be changed to  $x_n^{(u+R)L+v} = x_n^{u \times L+v}$  and  $x_n^{(u-1)L+v+L} = x_n^{(u-1)L+v}$ . All the node values in the converted model can be arranged as an  $(R \times L)$ -dimensional column vector,  $\mathbf{z}_n = [x_n^1, x_n^2, \dots, x_n^L, x_n^{L+1}, x_n^{L+2}, \dots, x_n^{2L}, \dots, x_n^{R \times L}]^T$ . Similarly to the method used for the 1D CML [39], one can differentiate Eq. (3) and evaluate the derivatives along their synchronized trajectories. Upon synchronization, all the entries of  $\mathbf{z}_n$  become equal, i.e.,  $x_n^1 = x_n^2 = \dots = x_n^L = x_n^{L+1} = x_n^{L+2} = \dots = x_n^{2L} = \dots = x_n^{R \times L} = x_n$ .

Along the synchronized trajectory, one has the derivatives of  $F$  as

$$\begin{aligned} F'(x_n^{(u-1)L+v}) &= F'(x_n^{u \times L+v}) = F'(x_n^{(u-2)L+v}) \\ &= F'(x_n^{(u-1)L+v+1}) = F'(x_n^{(u-1)L+v-1}) = F'(x_n), \end{aligned} \quad (4)$$

and the differentials of the 2D CML are

$$\begin{aligned} \delta(x_{n+1}^{(u-1)L+v}) &= (1-\varepsilon)F'(x_n^{(u-1)L+v})\delta(x_n^{(u-1)L+v}) \\ &\quad + \frac{\varepsilon}{4} [F'(x_n^{u \times L+v})\delta(x_n^{u \times L+v}) \\ &\quad + F'(x_n^{(u-2)L+v})\delta(x_n^{(u-2)L+v}) \\ &\quad + F'(x_n^{(u-1)L+v+1})\delta(x_n^{(u-1)L+v+1}) \\ &\quad + F'(x_n^{(u-1)L+v-1})\delta(x_n^{(u-1)L+v-1})]. \end{aligned} \quad (5)$$

By incorporating Eq. (4), Eq. (5) can be written as

$$\begin{aligned} \delta(x_{n+1}^{(u-1)L+v}) &= F'(x_n) [(1-\varepsilon)\delta(x_n^{(u-1)L+v}) \\ &\quad + \frac{\varepsilon}{4} (\delta(x_n^{u \times L+v}) + \delta(x_n^{(u-2)L+v}) \\ &\quad + \delta(x_n^{(u-1)L+v+1}) + \delta(x_n^{(u-1)L+v-1}))]. \end{aligned} \quad (6)$$

Applying Eq. (6) to all the  $(R \times L)$  elements produced at time instants  $(n+1)$  and  $n$ , i.e.,  $\mathbf{z}_{n+1}$  and  $\mathbf{z}_n$ , one can get a matrix form of Eq. (5), as,

$$\delta \mathbf{z}_{n+1} = \mathbf{J}_n \delta \mathbf{z}_n,$$

where  $\mathbf{J}_n$  is the Jacobin matrix satisfying  $\mathbf{J}_n = F'(x_n)\mathbf{K}$  and

$\mathbf{K}$  is an  $(R \times L) \times (R \times L)$  circulant matrix in the form of

$$\mathbf{K} = \begin{bmatrix} \mathbf{A}_1 & \mathbf{A}_2 & \cdots & \mathbf{A}_R \\ \mathbf{A}_R & \mathbf{A}_1 & \cdots & \mathbf{A}_{R-1} \\ \vdots & \vdots & \ddots & \vdots \\ \mathbf{A}_2 & \mathbf{A}_3 & \cdots & \mathbf{A}_1 \end{bmatrix}_{(R \times L) \times (R \times L)}.$$

Here, the matrices  $\mathbf{A}_1, \mathbf{A}_2, \dots, \mathbf{A}_R$  are given by

$$\begin{aligned} \mathbf{A}_1 &= \begin{bmatrix} 1-\varepsilon & \varepsilon/4 & 0 & \cdots & \varepsilon/4 \\ \varepsilon/4 & 1-\varepsilon & \varepsilon/4 & \ddots & 0 \\ 0 & \varepsilon/4 & 1-\varepsilon & \ddots & 0 \\ \vdots & \vdots & \ddots & \ddots & \varepsilon/4 \\ \varepsilon/4 & 0 & \cdots & \varepsilon/4 & 1-\varepsilon \end{bmatrix}_{L \times L}, \\ \mathbf{A}_2 = \mathbf{A}_R &= \begin{bmatrix} \varepsilon/4 & & & & \\ & \ddots & & & \\ & & \varepsilon/4 & & \\ & & & \ddots & \\ & & & & \varepsilon/4 \end{bmatrix}_{L \times L}, \end{aligned}$$

and

$$\mathbf{A}_3 = \mathbf{A}_4 = \cdots = \mathbf{A}_{R-1} = \begin{bmatrix} 0 & \cdots & 0 \\ \vdots & \ddots & \vdots \\ 0 & \cdots & 0 \end{bmatrix}_{L \times L}.$$

To calculate the LEs of the 2D CML, one needs to multiply all the Jacobin matrices. Let  $\lambda$  represent an eigenvalue of the matrix  $\mathbf{K}$  and denote  $\mathbf{G} = \mathbf{J}_1 \times \mathbf{J}_2 \times \cdots \times \mathbf{J}_n = \mathbf{K}^n \cdot (\prod_{m=1}^n F'(x_m))$ . It is easy to verify that the eigenvalue of  $\mathbf{G}$  is  $\lambda^n \cdot (\prod_{m=1}^n F'(x_m))$ . According to Eq. (2), the LEs of 2D CML are given by the following formula, parametrized by  $\lambda$ :

$$\begin{aligned} \text{LEs} &= \lim_{n \rightarrow \infty} \frac{1}{n} \ln |\mathbf{J}_1 \times \mathbf{J}_2 \times \cdots \times \mathbf{J}_n| \\ &= \lim_{n \rightarrow \infty} \frac{1}{n} \ln \left| \lambda^n \prod_{m=1}^n F'(x_m) \right| \\ &= \lim_{n \rightarrow \infty} \frac{1}{n} \ln \left| \prod_{m=1}^n F'(x_m) \right| + \ln |\lambda|. \end{aligned} \quad (7)$$

Note that the first term in Eq. (7) is precisely the LE of the local chaotic map  $F$ , that is,  $\lim_{n \rightarrow \infty} \frac{1}{n} \ln |\prod_{m=1}^n F'(x_m)| = \text{LE}_F$ . So, to calculate the LE of the 2D CML, one has to compute the second term  $\ln |\lambda|$ . Here,  $\lambda$  represents any eigenvalue of  $\mathbf{K}$  and  $\mathbf{K}$  is a block circulant matrix with most of the blocks being zero (i.e.,  $\mathbf{A}_3 = \cdots = \mathbf{A}_{R-1} = \mathbf{0}$ ). Its characteristic polynomial is [40]

$$\prod_{r=0}^{R-1} |\mathbf{A}_1 + \mathbf{A}_2 \omega_r + \mathbf{A}_R \omega_r^{R-1} - \lambda \mathbf{I}|, \quad (8)$$

where  $\mathbf{I}$  is the identity matrix and

$$\omega_r = \exp\left(i \frac{2\pi r}{R}\right) = \cos \frac{2\pi r}{R} + i \sin \frac{2\pi r}{R},$$

for  $r = 0, 1, \dots, R-1$ . Expanding the inner part of Eq. (8),

one gets

$$\mathbf{A} = \mathbf{A}_1 + \mathbf{A}_2 \omega_r + \mathbf{A}_R \omega_r^{R-1} - \lambda \mathbf{I}$$

$$= \begin{bmatrix} j & \varepsilon/4 & 0 & \cdots & \varepsilon/4 \\ \varepsilon/4 & j & \varepsilon/4 & \cdots & 0 \\ \vdots & \vdots & \vdots & \ddots & \vdots \\ \varepsilon/4 & 0 & 0 & \cdots & j \end{bmatrix}_{L \times L},$$

where  $j = 1 - \varepsilon + \frac{\varepsilon}{4} \omega_k + \frac{\varepsilon}{4} \omega_k^{R-1} - \lambda$ . It is clear that  $\mathbf{A}$  is still a circulant matrix. Applying the same technique as used above [40], one obtains

$$\lambda = 1 - \varepsilon + \frac{\varepsilon}{4} \omega_r + \frac{\varepsilon}{4} \omega_r^{R-1} + \frac{\varepsilon}{4} \mu_l + \frac{\varepsilon}{4} \mu_l^{L-1}, \quad (9)$$

where  $\mu_l = \exp\left(i \frac{2\pi l}{L}\right) = \cos \frac{2\pi l}{L} + i \sin \frac{2\pi l}{L}$ , with  $l = 0, 1, \dots, L-1$ .

Substitute Eq. (9) into Eq. (7) gives all the (R+L) LEs of 2D CML, i.e.,

$$\text{LEs} = \text{LE}_F + \ln \left| 1 - \varepsilon + \frac{\varepsilon}{2} \left( \cos \frac{2\pi r}{R} + \cos \frac{2\pi l}{L} \right) \right|, \quad (10)$$

for  $r = 0, 1, \dots, R-1$  and  $l = 0, 1, \dots, L-1$ . From this analytical formula, it is easy to get the following results.

**Theorem 1.** *The maximum Lyapunov exponent of the 2D CML model is determined by the local chaotic map F.*

*Proof.* According to Eq. (10), the maximum LE of 2D CML is given by  $\text{LE} = \text{LE}_F$ , when  $r = 0$  and  $l = 0$ .  $\square$

**Corollary 1.** *The maximum Lyapunov exponent is independent of the size of the 2D CML model.*

**Corollary 2.** *In 2D CML, increasing  $\text{LE}_F$  will increase the maximum Lyapunov exponent of the whole 2D lattice.*

### B. Pseudo-Randomness Extraction From the 2D CML

According to the above analyses, with appropriate selection of the local chaotic map F, the maximum Lyapunov exponent of the 2D CML will be positive and the orbits of the whole system will only run in fully developed chaotic state.

Given the initial conditionals of the 2D CML and the system parameters of F, if any, the distribution of the orbits is governed by a PRD<sup>1</sup>. Without loss of generality, assume that this PRD is not uniform. This is because only few local chaotic maps are known to have a uniform density, for example the tent map [41]. And, even if a uniform local map is used, the overall density is likely to be uneven after coupling the local maps together in the structure of 2D CML. Similarly to sampling a random variable from a true random distribution, the way of taking a sample from this PRD is to iterate the 2D CML.

The following discussion shows how to squeeze uniform bits from the non-uniform PRD that governs the 2D CML's orbits. This discussion starts with a general result that holds for both pseudo-random distribution and true random distribution.

**Theorem 2.** *For a random (or pseudo-random) distribution in  $[0, 1]$ , assume that the density function has bounded first-order derivative. For any sample  $x = 0.w_1 w_2 \cdots w_z$  ( $w_i \in \{0, 1\}$  and  $i \in [1, z]$ ) from this distribution, one has*

$$\lim_{z \rightarrow \infty} P(w_z = 0) = \lim_{z \rightarrow \infty} P(w_z = 1).$$

*Proof.* See the appendix.  $\square$

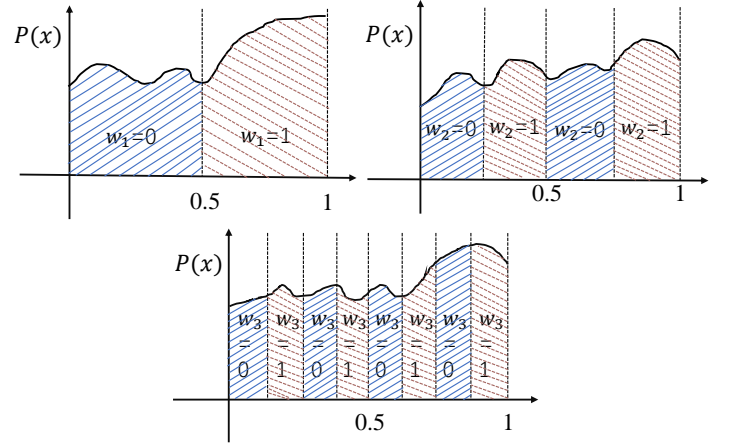


Fig. 2. Illustration of Theorem 2.

**Remark:** This theorem can be intuitively understood from the examples depicted in Fig. 2. For any (pseudo) random sample  $x \in [0, 1]$ , if there is only 1-bit ( $z = 1$ ) used to represent this number, then the difference of the probabilities of  $P(w_1 = 0)$  and  $P(w_1 = 1)$  equals the difference of the areas associated with the two slices in blue and red (as shown in the top-left of Fig. 2). As  $z$  goes larger (for example,  $z = 2$  and  $z = 3$  in Fig. 2), the slices become smaller and their associated areas become similar. Thus, from the appendix, it is easy to see that  $|P(w_z = 0) - P(w_z = 1)| = O(2^{-z})$ .

**Remark:** Although the theorem is proved by assuming that the density function has a bounded first-order derivative, which implies continuity, it can be easily extended to a density with countably many points of discontinuity, which is always the case of finite precision representations of real chaotic orbits.

Theorem 2 states the fact that, under fixed-point arithmetic, the farther away from the radix point, the more uniform the bits tend to be. For a given PRD determined by a 2D CML instance, a naive way of using Theorem 2 to extract (pseudo) random bits is to take the rightmost bit of a chaotic orbit under finite precision representation. If the precision is  $z$  bit, a single uniform bit with bias bounded by  $O(2^{-z})$  can be obtained from one orbit. However, as discussed in Sec. I, the efficiency of this method is too low to meet practical requirements. Nevertheless, as will be seen in the following, this drawback can be avoided by making use of more CML instances and Property 1 given below.

For two different 2D CML instances, assume that their associated initial conditions and system parameters are selected independently. Consequently, the associated PRDs induced by these two instances are independent of each other, and so do the pseudo-random samples drawn from the two PRDs. For

<sup>1</sup>This kind of chaotic system is referred to as a 2D CML instance.

any sample  $x = 0.x_1x_2 \cdots x_z$  drawn from the first PRD and  $y = 0.y_1y_2 \cdots y_z$  drawn from the second PRD, by letting  $w = x_i + y_j \pmod{2}$ , one can conclude that  $w$  is more uniform than both  $x_i$  and  $y_j$  ( $i, j \in [1, z]$ ). Specifically, the bias of  $w$  is bounded by  $O(2^{-(i+j)})$ , as shown below.

**Property 1.** *Let  $x_i$  and  $y_j$  be independent binary random bits with bounded bias  $O(2^{-i})$  and  $O(2^{-j})$ , respectively. Then,  $w = x_i + y_j \pmod{2}$  satisfies*

$$|P(w = 0) - P(w = 1)| = O(2^{-(i+j)}).$$

*Proof.* See the appendix.  $\square$

Extending this property further, the following corollary can be easily obtained. From this corollary, it is easy to see that, with more independent PRDs, one can obtain bits with arbitrarily small bias.

**Corollary 3.** *Let  $w_1, w_2, \dots, w_c$  be  $c$  mutually independent binary random variables, and each with bounded bias  $O(2^{-k_i})$  ( $i \in [1, c]$ ), and set  $w = \sum_{i=1}^c w_i \pmod{2}$ . Then, one has*

$$|P(w = 0) - P(w = 1)| = O(2^{-(\sum_{i=1}^c k_i)}).$$

Property 1 holds only when the samples  $x$  and  $y$  are drawn from independent (pseudo) random distributions, which requires the two CML instances be selected independently. By making use of the result about LE in Sec. III-A, this assumption can be further relaxed. If the initial conditions or the system parameters of the CML instances are correlated but they both have large positive LE, then the correlation between their orbits will be dispersed fast after a few iterations. This transition period can be determined by applying the independence test from Sec. II-D to the orbits. In this way, the choice of the two 2D CML instances can be made arbitrary if both CMLs have large positive LEs and the orbits in transition are discarded.

Based on the discussion above, one can improve the efficiency of pseudo-random bits generation for  $z$  times by using two 2D CML instances, while keeping the bias be  $O(2^{-z})$ . The end-to-end extraction Algorithm 1 summarizes the details.

#### IV. EXPERIMENTAL ANALYSIS

In this section, numeric tests are carried out on different 2D CML systems to assess the applicability and performance of the theoretic results developed in Sec. III. Some popular chaotic systems are used as the local map F of Eq. (1)

- The Logistic map

$$x_{n+1} = \mu x_n(1 - x_n),$$

where  $\mu \in (0, 4]$  and  $x_n \in (0, 1)$ .

- The Tent map

$$x_{n+1} = \begin{cases} \mu x_n, & \text{if } x_n \in (0, 0.5), \\ \mu(1 - x_n), & \text{if } x_n \in [0.5, 1), \end{cases}$$

where  $\mu \in (0, 2]$  is the system parameter.

---

#### Algorithm 1: Extraction Algorithm E

---

**Input:** Two sets of initial conditions and system parameters 2D CML.

**Output:** Pseudo-random bits.

**Function** ModAdd( $x, y$ ):

```

 $x = 0.x_1x_2 \cdots x_z$ 
 $y = 0.y_1y_2 \cdots y_z$ 
 $w = w_1w_2 \cdots w_z$ 
 $w_i = x_i + y_{z+1-i} \pmod{2}$ 
return  $w$ 
```

**Function** Main:

```

Step 1 Run the two CML instances and collect
their corresponding orbits  $\{x^i\}_{i=0}^K$  and  $\{y^i\}_{i=0}^K$ ,
and update the states
Step 2 Perform the independence test on the
collected orbits
if test passed then
    while necessary do
        Run the two instances to get  $(x^0, y^0)$ 
        ModAdd( $x^0, y^0$ )
    end
else
    go back to Step 1
end
return 0
```

---

- The piecewise Logistic map (PLM)

$$x_{n+1} = \begin{cases} \mu N^2(x_n - \frac{i-1}{N})(\frac{i}{N} - x_n), & \text{if } \frac{i-1}{N} < x_n < \frac{i}{N}, \\ 1 - \mu N^2(x_n - \frac{i-1}{N})(\frac{i+1}{N} - x_n), & \text{if } \frac{i}{N} < x_n < \frac{i+1}{N}, \end{cases}$$

where  $\mu \in (0, 4]$  is the system parameter and  $N$  is the number of segments.

It is worth mentioning that, other than the basic ones listed here, chaotic maps with more complex behavior, such as the ones suggested in [13, 14], can also be employed as the local map of the 2D CML system. For simplicity, refer the resultant chaotic systems to as L-CML, T-CML, and PLM-CML, respectively.

##### A. Lyapunov Exponents and Bifurcation Diagrams

In this section, it is verified that the theoretic LE formula (10) of the 2D CML is correct. Then, the associated bifurcation diagram is used to demonstrate that the orbits of the CML instance indeed run in full chaotic state with appropriate parameters.

The reliable Wolf's scheme [34] is used to calculate the LEs of the 2D CML, and the result is plotted in Fig. 3 with  $\mu = 4, 2, 4$  for L-CML, T-CML and PLM-CML, respectively. Here, the other parameters in Eq. (1) are set to  $\varepsilon = 0.1$ ,  $R = L = 8$ , and the number of segments of PLM  $N = 64$ . It is clear that the theoretic scheme given by Eq. (10) perfectly aligns with the numeric method.



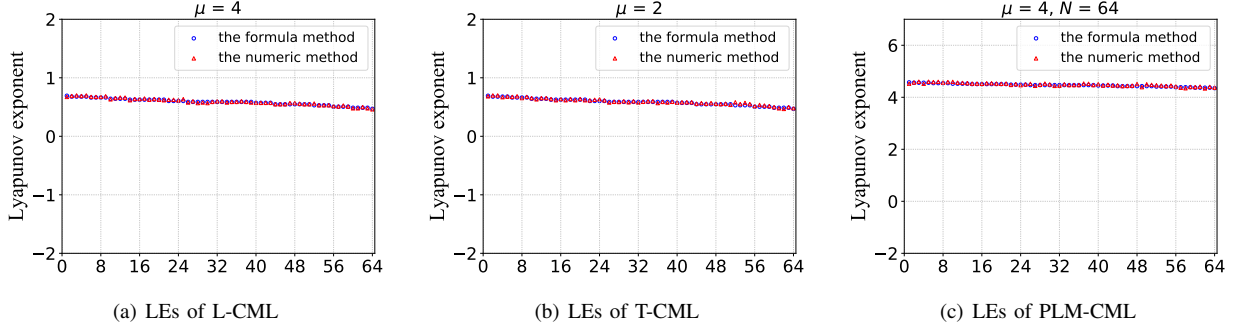


Fig. 3. LEs obtained from the numeric method in [34] and theoretic result in Eq. (1).

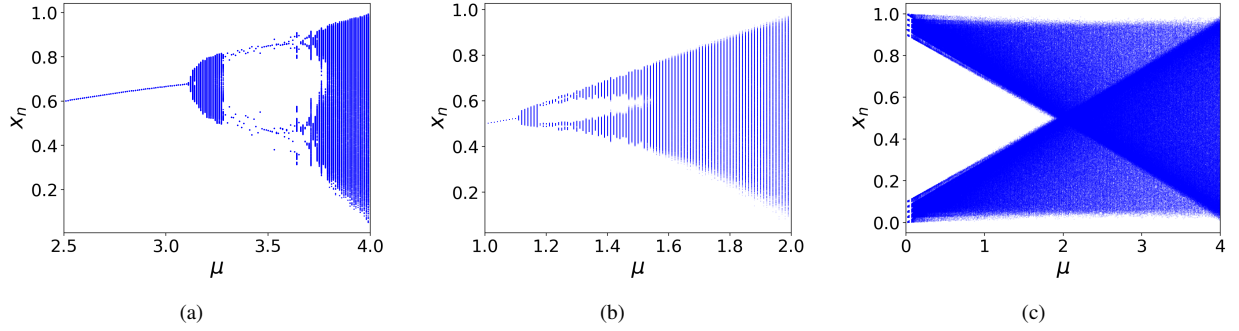


Fig. 4. Bifurcation diagram corresponding to the first node of L-CML, T-CML and PLM-CML, respectively.

To demonstrate of chaos, the bifurcation diagram is used to plot output orbits of the system with respect to the change of the parameters. As shown in Theorem 1, the maximum LE of a 2D CML is solely determined by the local map  $LE_F$ . And, the orbits extracted from the first node (i.e.,  $r = l = 0$  in Eq. (1)) achieves the maximum LE. By varying the parameter  $\mu$ , one can exact the orbits of the first node of L-CML, T-CML, and PLM-CML, respectively, and their bifurcation diagrams are shown in Fig. 4. It is clear that the orbits of CML run in the chaotic state with an appropriate choice of the parameter of the local map. Once again, it should be pointed out that, with more complex chaotic systems, the  $LE_F$  can be made larger [13, 14], and the resulting chaotic performance will be better. This may bring up more benefits like a higher extraction rate of the pseudo-random numbers, but such possible improvement is left for future study. Moreover, other metrics, such as Kolmogorov entropy, fractal power spectra and correlation dimension, can be used to measure the performance of chaos, which likewise not the focus of this study.

### B. Randomness Tests

To assess the results presented in Sec. III-B, the pseudo-random distributions introduced by L-CML, T-CML and PLM-CML are first plotted. Under the same parameter settings, the resulting distributions are shown in Fig. 5. Note that the distribution of the Tent map is known to be uniform when  $\mu = 2$  [41], but similarly to that of L-CML and PLM-CML, the distribution of T-CML is not uniform. This observation corroborates the discussion in Sec. I, implying that

a theoretically sound method for squeezing random number from the chaotic orbits is desirable.

Next, statistical tests are performed on binary outputs of the extraction algorithm **E**. The parameter settings are the same as above, while the precision  $z$  is set to 64 and the parameter  $K$  for the independence test is set to  $10^3$ . With 3 local maps, there are  $3 \times 3 = 9$  pairs of 2D CML instances as the input of **E**. For each pair, one of the initial conditions of the CML instance is set to random and the other is obtained by perturbing the first one with difference up to  $10^{-3}$ . Note that the initial conditions are strongly correlated, so this is the worst-case study for the extraction algorithm **E**. But, as argued in Sec. III-B, positive LE can disperse the correlation within initial conditions. After a transition period, the resultant orbits (and thus PRD) are pseudo-independent of each other. The binary outputs are collected and tested against NIST SP800-22 [31] and TestU01 [32].

**NIST SP800-22:** This is a statistical randomness test suite for binary sequences. It is a collection of 15 tests, each of them outputs one (or, in a few cases, more than one)  $P$ -value. The suite is designed to be applied over binary sequences with length  $10^6$ . The significance level  $\alpha$ , which determines the region of acceptance of the assumption that the sequence being tested is random, is suggested to be set to 0.01. A sequence passes a test if  $P$ -value is not less than  $\alpha$ .

Each test is designed such that the probability for an ideal generator to fail a test is  $\alpha$ . So,  $1000 > 1/\alpha$  sequences with length  $10^6$  produced by the extraction algorithm **E** are considered and tested. According to [31, Chap. 4], empirical test results with  $P$ -value  $\geq \alpha$  should be examined further ac-

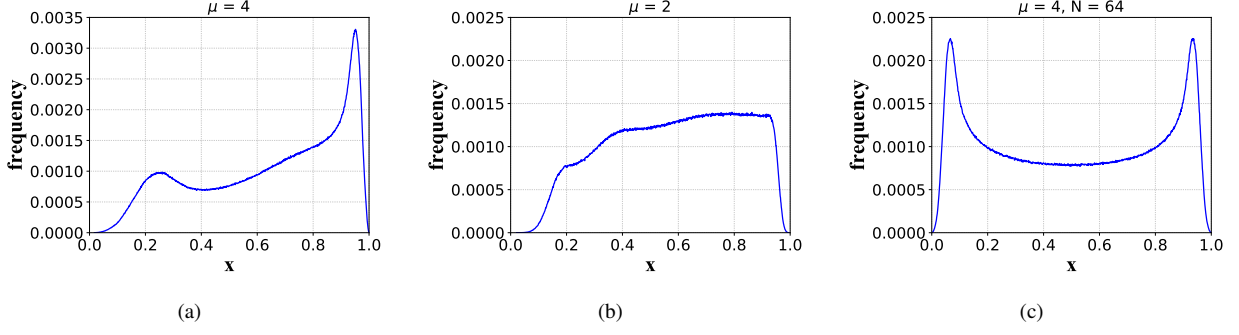


Fig. 5. Orbits distribution of L-CML, T-CML and PLM-CML, respectively.

cording to<sup>2</sup>: 1) the pass rate of the sub-tests; 2) the distribution of empirical  $P$ -values. The pass rate is approximated with a normal random variable, and under the current setting, a pass rate  $< 0.98056$  is interpreted as evidence of non-randomness. The 1000  $P$ -values from each sub-test will be further tested against a chi-square goodness-of-fit test with 10 bins, and this again produces another  $P$ -value<sub>T</sub> (i.e., a  $P$ -value of  $P$ -values). If  $P$ -value<sub>T</sub>  $\geq 0.0001$ , the sequences are considered to be uniform.

**TestU01:** Generally speaking, it is a more systematic test suite for random numbers. TestU01 works for both random number over the interval  $(0, 1)$  and binary sequences, and it contains six predefined batteries of tests. In this work, the batteries *Rabbit*, *Alphabit* and *BlockAlphabit* designed for binaries are selected. The batteries *Rabbit* and *Alphabit* have 38 and 17 statistical sub-tests, and *BlockAlphabit* applies the sub-tests in *Alphabit* repeatedly after reordering the bits by a block length specified by the software package. This test suite is run on binary sequences with length  $2^{20}$ ,  $2^{25}$  and  $2^{30}$ , and a  $P$ -value lies outside the range  $[0.001, 0.999]$  is interpreted as fail; otherwise, it passes.

Taking two correlated L-CML instances as input, **E** produces  $10^3 \times 10^6$  bits and these bits are tested against NIST 800-22. Table I shows the results of each sub-test of NIST 800-22, where the two-level testing procedure discussed above is applied. Note that the  $P$ -value displayed here is just a typical test output. It is clear that the output of the extraction algorithm **E** passes the NIST 800-22 test. Similarly, taking two correlated T-CML instances as input, the TestU01 test suite is run on the outputs and the results are summarized in Table II. Clearly, the output of the extraction algorithm **E** also passes the TestU01 test. Moreover, all other 8 pairs of input of **E** pass both NIST 800-22 and TestU01 tests, but the results are omitted here due to space limitation. The experimental results confirm that the developed theory provides a sound foundation for generating pseudo-random bits from digital chaos and the extraction algorithm **E** can be used to produce uniform bits for secure applications.

## V. CONCLUSION

Coupling chaotic maps is a common strategy to generate more complex dynamic behavior, using for example 1D and

TABLE I  
NIST 800-22 TEST RESULTS ON **E** WITH TWO CORRELATED L-CML INSTANCES AS INPUT.

Sub-test	$P$ -value <sup>†</sup>	Pass Rate	$P$ -value <sub>T</sub>
	$\geq 0.01$	$\geq 0.98056$	$\geq 0.0001$
Frequency	0.8902	0.9890	0.8677
Block Freq.	0.7511	0.9890	0.9179
Cumulative*	0.3775	0.9860	0.1835
Runs	0.1881	0.9900	0.0242
Longest Run	0.9101	0.9930	0.6931
Rank	0.5842	0.9900	0.1381
Spectral (FFT)	0.6464	0.9890	0.5341
Nonoverlap*	0.4994	0.9895	0.4702
Universal	0.8006	0.9820	0.0669
App. Entropy	0.4894	0.9830	0.4245
Random E.*	0.3198	0.9893	0.5463
Random E. V.*	0.3176	0.9915	0.4760
Serial*	0.2898	0.9880	0.3429
Linear Comp.	0.4376	0.9870	0.1581
Success Counts	15/15	15/15	15/15

\* These tests generates more than one  $P$ -values; † Only one of the test results has been considered in the table.

TABLE II  
TESTU01 TEST RESULTS ON **E** WITH TWO CORRELATED T-CML INSTANCES AS INPUT.

Length	<i>Rabbit</i>	<i>Alphabit</i>	<i>BlockAlphabit</i>
$2^{30}$	38/38	17/17	17/17
$2^{25}$	38/38	17/17	17/17
$2^{20}$	38/38	17/17	17/17

2D coupled map lattices in secure communications. This work presents the first theoretic study of the Lyapunov exponents of the 2D CML model and finds that the maximum LE is solely determined by the local map used for coupling. Moreover, by bridging true randomness and pseudo-randomness, it lays the theoretic foundation for the distribution of the digitized chaotic orbits. Making use of this result, a random number extraction algorithm **E** is designed, which produces pseudo-random bits with bias bounded by  $O(2^{-z})$ , where  $z$  is the bit number of the precision. Extensive experiments are carried out and the results align perfectly with the theoretic formulas. The

<sup>2</sup>This is called the two-level random number testing procedure [42].



theory may give new insights for using chaos to obtain pseudo-randomness. More efficiency improvements of the chaotic random number generator and theoretical study of pseudo-random distribution induced by chaos will be carried out in future work.

## APPENDIX PROOF OF THEOREM 2 AND PROPERTY 2

*Proof.* Let  $P(x)$  be the density function of  $x \in [0, 1]$ , which bounds the first derivative  $P'(x)$ . Considering that  $x$  is represented with  $z$  bits, one has  $P(w_z = 0) + P(w_z = 1) = 1$  and

$$P(w_z = 0) = \sum_{b=1}^{2^{z-1}} \int_{\frac{2(b-1)}{2^z}}^{\frac{2b-1}{2^z}} P(x) dx, \quad (11)$$

$$P(w_z = 1) = \sum_{b=1}^{2^{z-1}} \int_{\frac{2b-1}{2^z}}^{\frac{2b}{2^z}} P(x) dx. \quad (12)$$

Applying the mean-value theorem to Eqs. (11) and (12), one gets

$$\begin{aligned} P(w_z = 0) &= \sum_{b=1}^{2^{z-1}} \int_{\frac{2(b-1)}{2^z}}^{\frac{2b-1}{2^z}} P(x) dx \\ &= \int_0^{\frac{1}{2^z}} P(x) dx + \int_{\frac{1}{2^z}}^{\frac{2}{2^z}} P(x) dx + \dots \\ &\quad + \int_{\frac{2^{z-2}}{2^z}}^{\frac{2^{z-1}-1}{2^z}} P(x) dx \\ &= \frac{1}{2^z} [P(x_1) + P(x_2) + \dots + P(x_{2^{z-1}})], \end{aligned}$$

where  $\frac{2(i-1)}{2^z} \leq x_i \leq \frac{2i-1}{2^z}$  for  $i \in [1, 2^{z-1}]$ , and similarly,

$$\begin{aligned} P(w_z = 1) &= \sum_{b=1}^{2^{z-1}} \int_{\frac{2b-1}{2^z}}^{\frac{2b}{2^z}} P(x) dx \\ &= \frac{1}{2^z} [P(x'_1) + P(x'_2) + \dots + P(x'_{2^{z-1}})], \end{aligned}$$

where  $\frac{2i-1}{2^z} \leq x'_i \leq \frac{2i}{2^z}$  for  $i \in [1, 2^{z-1}]$ . Finally, one has

$$\begin{aligned} &\lim_{z \rightarrow \infty} |P(w_z = 1) - P(w_z = 0)| \\ &\leq \lim_{z \rightarrow \infty} \frac{1}{2^z} \left( \sum_{i=1}^{2^{z-1}} |P(x_i) - P(x'_i)| \right) \\ &\leq \lim_{z \rightarrow \infty} \frac{1}{2^z} \cdot \left( \sum_{i=1}^{2^{z-1}} |P'(\bar{x}_i)| \cdot \frac{2}{2^z} \right) \\ &\leq \lim_{z \rightarrow \infty} \frac{1}{2^z} \cdot (2^{z-1} \max |P'(\bar{x}_i)|) \cdot \frac{2}{2^z} \\ &\leq \lim_{z \rightarrow \infty} \frac{1}{2^z} \cdot (\max |P'(\bar{x}_i)|) \\ &= 0, \end{aligned} \quad (13)$$

where  $\bar{x}_i \in (x_i, x'_i)$  and Eq. (13) is derived based on the mean value theorem.  $\square$

*Proof.* By assumption, one has

$$\begin{aligned} |P(x_i = 0) - P(x_i = 1)| &= O(2^{-i}), \\ |P(y_j = 0) - P(y_j = 1)| &= O(2^{-j}). \end{aligned}$$

Since  $w = x_i + y_j \pmod{2}$  and  $x_i$  and  $y_j$  are independent of each other, one gets

$$\begin{aligned} P(w = 0) &= P(x_i = 0)P(y_j = 0) + P(x_i = 1)P(y_j = 1), \\ P(w = 1) &= P(x_i = 0)P(y_j = 1) + P(x_i = 1)P(y_j = 0). \end{aligned}$$

The bias of  $w$  can then be calculated as

$$\begin{aligned} &|P(w = 0) - P(w = 1)| \\ &= |P(x_i = 0)P(y_j = 0) + P(x_i = 1)P(y_j = 1) \\ &\quad - P(x_i = 0)P(y_j = 1) - P(x_i = 1)P(y_j = 0)| \\ &= |[P(x_i = 0) - P(x_i = 1)] \cdot [P(y_j = 0) - P(y_j = 1)]| \\ &= O(2^{-(i+j)}). \end{aligned}$$

Hence, the property is true.  $\square$

## REFERENCES

- [1] G. Jakimoski and L. Kocarev, "Chaos and cryptography: Block encryption ciphers based on chaotic maps," *IEEE Trans. Circuits Syst. I-Fundam. Theor. Appl.*, vol. 48, no. 2, pp. 163–169, 2001.
- [2] T. Yang, C. W. Wu, and L. O. Chua, "Cryptography based on chaotic systems," *IEEE Trans. Circuits Syst. I-Fundam. Theor. Appl.*, vol. 44, no. 5, pp. 469–472, 1997.
- [3] L. Kocarev, "Chaos-based cryptography: A brief overview," *IEEE Circuits Syst. Mag.*, vol. 1, no. 3, pp. 6–21, 2001.
- [4] P. Bergamo, P. D'Arco, A. De Santis, and L. Kocarev, "Security of public-key cryptosystems based on chebyshev polynomials," *IEEE Trans. Circuits Syst. I-Regul. Pap.*, vol. 52, no. 7, pp. 1382–1393, 2005.
- [5] S. El Assad, M. Farajallah, and C. Vlădeanu, "Chaos-based block ciphers: An overview," in *2014 10th International Conference on Communications (COMM)*. IEEE, 2014, pp. 1–4.
- [6] L. Y. Zhang, Y. Liu, F. Pareschi, Y. Zhang, K.-W. Wong, R. Rovatti, and G. Setti, "On the security of a class of diffusion mechanisms for image encryption," *IEEE Trans. Cybern.*, vol. 48, no. 4, pp. 1163–1175, 2017.
- [7] G. Alvarez, F. Montoya, M. Romera, and G. Pastor, "Breaking two secure communication systems based on chaotic masking," *IEEE Trans. Circuits Syst. II: Exp. Briefs*, vol. 51, no. 10, pp. 505–506, 2004.
- [8] Z. Hua and Y. Zhou, "One-dimensional nonlinear model for producing chaos," *IEEE Trans. Circuits Syst. I-Regul. Pap.*, vol. 65, no. 1, pp. 235–246, 2017.
- [9] X. Cao, L. Du, X. Wei, D. Meng, and X. Guo, "High capacity reversible data hiding in encrypted images by patch-level sparse representation," *IEEE Trans. Cybern.*, vol. 46, no. 5, pp. 1132–1143, 2015.
- [10] A. Miranian and M. Abdollahzade, "Developing a local least-squares support vector machines-based neuro-fuzzy model for nonlinear and chaotic time series prediction," *IEEE Trans. Neural Netw. Learn. Syst.*, vol. 24, no. 2, pp. 207–218, 2012.
- [11] Y. Wang, Z. Liu, J. Ma, and H. He, "A pseudorandom number generator based on piecewise logistic map," *Nonlinear Dyn.*, vol. 83, no. 4, pp. 2373–2391, 2016.
- [12] Y. Zhou, Z. Hua, C.-M. Pun, and C. P. Chen, "Cascade chaotic system with applications," *IEEE Trans. Cybern.*, vol. 45, no. 9, pp. 2001–2012, 2014.
- [13] Z. Hua, S. Yi, Y. Zhou, C. Li, and Y. Wu, "Designing hyper-chaotic cat maps with any desired number of positive lyapunov exponents," *IEEE Trans. Cybern.*, vol. 48, no. 2, pp. 463–473, 2017.

- [14] Z. Hua and Y. Zhou, "Dynamic parameter-control chaotic system," *IEEE Trans. Cybern.*, vol. 46, no. 12, pp. 3330–3341, 2015.
- [15] Z. Li, C. Peng, L. Li, and X. Zhu, "A novel plaintext-related image encryption scheme using hyper-chaotic system," *Nonlinear Dyn.*, vol. 94, no. 2, pp. 1319–1333, 2018.
- [16] F. Dachselt and W. Schwarz, "Chaos and cryptography," *IEEE Trans. Circuits Syst. I-Regul. Pap.*, vol. 48, no. 12, pp. 1498–1509, 2001.
- [17] P. Li, Z. Li, W. A. Halang, and G. Chen, "A multiple pseudorandom-bit generator based on a spatiotemporal chaotic map," *Phys. Lett. A*, vol. 349, no. 6, pp. 467–473, 2006.
- [18] X. Lv, X. Liao, and B. Yang, "A novel pseudo-random number generator from coupled map lattice with time-varying delay," *Nonlinear Dyn.*, vol. 94, no. 1, pp. 325–341, 2018.
- [19] Q. Wang, S. Yu, C. Li, J. Lü, X. Fang, C. Guyeux, and J. M. Bahi, "Theoretical design and FPGA-based implementation of higher-dimensional digital chaotic systems," *IEEE Trans. Circuits Syst. I-Regul. Pap.*, vol. 63, no. 3, pp. 401–412, 2016.
- [20] Y. Wang, K.-W. Wong, and D. Xiao, "Parallel hash function construction based on coupled map lattices," *Commun. Nonlinear Sci. Numer. Simul.*, vol. 16, no. 7, pp. 2810–2821, 2011.
- [21] S. Coombes and A. H. Osbaldestin, "Period-adding bifurcations and chaos in a periodically stimulated excitable neural relaxation oscillator," *Phys. Rev. E*, vol. 62, no. 3, p. 4057, 2000.
- [22] S. Kumar, M. Kumar, R. Budhiraja, M. Das, and S. Singh, "A cryptographic model for better information security," *J. Inf. Secur. Appl.*, vol. 43, pp. 123–138, 2018.
- [23] K.-W. Wong, B. S.-H. Kwok, and W.-S. Law, "A fast image encryption scheme based on chaotic standard map," *Phys. Rev. A*, vol. 372, no. 15, pp. 2645–2652, 2008.
- [24] X.-Q. Fu, B.-C. Liu, Y.-Y. Xie, W. Li, and Y. Liu, "Image encryption-then-transmission using DNA encryption algorithm and the double chaos," *IEEE Photonics J.*, vol. 10, no. 3, pp. 1–15, 2018.
- [25] I. Hussain, J. Ahmed, and A. Hussain, "An image encryption technique based on coupled map lattice and one-time S-boxes based on complex chaotic system," *J. Intell. Fuzzy Syst.*, vol. 29, no. 4, pp. 1493–1500, 2015.
- [26] Y. Wang, X. Liao, D. Xiao, and K.-W. Wong, "One-way hash function construction based on 2D coupled map lattices," *Inf. Sci.*, vol. 178, no. 5, pp. 1391–1406, 2008.
- [27] Y.-Q. Zhang and X.-Y. Wang, "A symmetric image encryption algorithm based on mixed linear-nonlinear coupled map lattice," *Inf. Sci.*, vol. 273, pp. 329–351, 2014.
- [28] M. E. Newman and M. Girvan, "Finding and evaluating community structure in networks," *Phys. Rev. E*, vol. 69, no. 2, p. 026113, 2004.
- [29] K. Kaneko, "Pattern dynamics in spatiotemporal chaos: Pattern selection, diffusion of defect and pattern competition intermittency," *Physica D*, vol. 34, no. 1-2, pp. 1–41, 1989.
- [30] S. Biswas and A. Das, "Patterns, bifurcations, multistability and hysteresis in an inhomogeneous coupled map lattice," *Int. J. Bifurcation and Chaos.*, vol. 26, no. 03, p. 1630008, 2016.
- [31] L. E. Bassham III, A. L. Rukhin *et al.*, *A Statistical Test Suite for Random and Pseudorandom Number Generators for Cryptographic Applications*. National Institute of Standards & Technology (NIST) Special Publication 800-22, Rev. 1a, 2010.
- [32] P. L'Ecuyer and R. Simard, "Testu01: A C library for empirical testing of random number generators," *ACM Transactions on Mathematical Software (TOMS)*, vol. 33, no. 4, pp. 1–40, 2007.
- [33] K. Kaneko, "Overview of coupled map lattices," *Chaos*, vol. 2, no. 3, pp. 279–282, 1992.
- [34] A. Wolf, J. B. Swift, H. L. Swinney, and J. A. Vastano, "Determining Lyapunov exponents from a time series," *Physica D*, vol. 16, no. 3, pp. 285–317, 1985.
- [35] C. E. Shannon, "Communication theory of secrecy systems," *Bell System Tech. J.*, vol. 28, no. 4, pp. 656–715, 1949.
- [36] L. Nian-Sheng, "Pseudo-randomness and complexity of binary sequences generated by the chaotic system," *Commun. Nonlinear Sci. Numer. Simul.*, vol. 16, no. 2, pp. 761–768, 2011.
- [37] J. von Neumann, "Various techniques used in connection with random digits," *Appl. Math Ser.*, vol. 12, no. 36-38, p. 5, 1951.
- [38] L. Devroye, "Sample-based non-uniform random variate generation," in *Proceedings of the 18th Conference on Winter Simulation*, 1986, pp. 260–265.
- [39] M. Ding and W. Yang, "Stability of synchronous chaos and on-off intermittency in coupled map lattices," *Phys. Rev. E*, vol. 56, no. 4, p. 4009, 1997.
- [40] H. Wang and X. Guo, "Characteristic polynomials and spectra of some block circulant graphs," *Polycycl. Aromat. Compd.*, vol. 33, no. 2, pp. 83–96, 2013.
- [41] J. Heidele, "The existence of periodic orbits of the tent map," *Phys. Lett. A*, vol. 143, no. 4-5, pp. 195–201, 1990.
- [42] F. Pareschi, R. Rovatti, and G. Setti, "On statistical tests for randomness included in the NIST SP800-22 test suite and based on the binomial distribution," *IEEE Trans. Inf. Forensic Secur.*, vol. 7, no. 2, pp. 491–505, 2012.